A Design Methods for Particle Dampers in Low Frequency Horizontal Free Vibrations

Niklas Joachim Meyer* and Robert Seifried*
Institute of Mechanics and Ocean Engineering, Hamburg University of Technology, Hamburg, Germany, www.tuhh.de/mum, n.meyer@tuhh.de, robert.seifried@tuhh.de

Summary. Particle dampers show a huge potential to efficiently damp lightweight structures. However, they suffer from their nonlinear characteristics and the multitude of influence parameters. For horizontal vibrations of low frequency, recently, the rolling attribute of spheres has been used to obtain high energy dissipation rates in driven particle containers. As long as the particle container's acceleration amplitude stays below the gravitational acceleration, this rolling effect of spheres can be used. Hereby, the estimation of the damper's energy dissipation is accurately possible using analytical formulas.
In this paper, a design guideline for a systematic damper design for an underlying structure of low first eigenfrequency under free vibration is presented. To develop this guideline, the analytical expression of the rolling effect of spheres is analyzed in detail. The particle damper is separated into multiple layers with different lengths. Hence, a high damping ratio over a large vibration amplitude range can be obtained. For experimental validation purposes, a simple beam-like structure is utilized. A good agreement between expected and experimental obtained vibration response is achieved for the designed particle dampers.

Introduction

To reduce large vibrations amplitudes of lightweight structures, passive damping techniques are often used. Classical liquid dampers are commonly utilized for these applications. Those dampers are well studied and mathematically easy to describe. However, liquid dampers fail under harsh environmental conditions and do need an anchor point. Thus, for applications where liquid dampers are not suitable, alternative damping technologies are necessary. Hence, *particle dampers* are an alternative, due to their simple and robust design.
Particle damping technology uses containers that are attached to the vibrating structure and are filled with granular material. By structural vibrations, momentum is transferred to the granular material which start to interact with each other. Due to these interactions, energy is dissipated by impacts and frictional phenomena between the particles. Particle dampers show great advantages compared to other damping technologies, as these add only little mass to the primary system [4], are cost-efficient devices, and might be applied to a wide frequency range [2]. Particle dampers can also be applied in harsh environmental conditions [14, 18]. One popular example are spacecraft applications [13]. Despite particle damper's huge potential, their design is still a non-trivial and challenging task. This is because particle motion, also called *motion mode*, and the damper's energy dissipation correlate in a non-trivial way, which is often poorly understood. Identifying these correlations is still part of ongoing research, see e. g. [3, 6, 7, 16, 19, 20, 21].
Especially, for low frequency vibrations, the use of particle dampers is rarely seen so far. For these vibrations, the particle container's acceleration amplitude is mostly below the gravitational acceleration. Hence, particles begin to stick and no relative motion between particles and container is obtained. Thus, only a little amount of energy is dissipated [5]. To face this problem, recently, in [12] the rolling attribute of spheres is studied for horizontal vibrations. It is shown that for low filling ratios, particles begin to slide and roll over the container base instead of sticking. For vibration amplitudes below a certain threshold stroke, which only depends on the filling ratio of the damper, no synchronous particle motion is obtained. This motion is named *scattered state*. The scattered state results in a comparatively low energy dissipation. Increasing the amplitude of the vibration above the threshold stroke, a synchronous particle motion with the container is obtained. The particles start to move as one particle block and collide inelastically with the container walls. This results in high energy dissipation rates and is called *rolling collect-and-collide* motion mode. For both observed motion modes, in [12] analytical equations are derived describing the damper's energy dissipation. These analytical equations are validated by comparison to experimental measurements of a driven particle container.
In this paper, the damper design of [12] is adopted to damp a structure of low first eigenfrequency under free vibration. Therefore, the analytical equations are studied in detail and a simple design guideline is derived. The idea of the design guideline is to separate the particle damper into multiple layers with different lengths. Hence, different vibration amplitudes can be damped efficiently, leading to high damping ratios on a large amplitude range. For validation purposes, a simple beam-like structure is utilized. The base point of the beam is fixed. The particle damper is mounted at the tip of the beam and the damper's velocity is measured using a laser scanning vibrometer. Thus, the system's free response is measured.
This paper is organized as follows: First, in Sect. **Motion Modes** the occurring motion modes for low-intensity horizontal vibrations are introduced. In the following Sect. **Design Guideline**, the particle damper's design guideline is developed. Then, in Sect. **Experimental Validation** the design guideline is applied to design a particle damper for the free vibration attenuation of a simple beam-like structure. Finally, a conclusion is given.

Motion Modes

A motion mode describes the motion of a particle bed inside a harmonic vibrating container of the form $x_c = X \sin(\Omega t)$, with container amplitude X and angular frequency $\Omega = 2\pi f$. For such a container movement, the corresponding container velocity and acceleration follow to $\dot{x}_c = V \cos(\Omega t)$ and $\ddot{x}_c = -A \sin(\Omega t)$ with $V = X \Omega$ and $A = X \Omega^2$. For such a container movement, different motion modes of the particle bed can be observed. Various influence parameters affect the occurring motion mode, like excitation intensity and frequency but also gravity, excitation direction, or particle size. The most common motion modes are solid-like, local fluidization, global fluidization, convection, Leidenfrost effect, bouncing collect-and-collide, and buoyancy convection [3, 6, 7, 16, 19, 20, 21].

For horizontal vibrations of low acceleration amplitude, i. e. $A < g$ with g being the gravitational acceleration, two different motion modes can be observed if spherical particles on flat container bases with low filling ratio are used, see [12] for a detailed discussion. An example of such a container is shown in Fig. 4 in form of the later utilized particle damper. The observed motion modes inside this container are called scattered and rolling collect-and-collide and are depicted schematically in Fig. 1. Particle trajectories of these two motion modes, obtained by discrete element simulations, are shown in Fig. 2 [12]. Interestingly, both motion modes only depend on the so-called optimal stroke X_{opt}, which only depends on the clearance h, i. e. the distance of the particle bed to the opposite container wall as indicated in Fig. 1. Following [12], the optimal stroke is obtained to

$$X_{\text{opt}} \approx 0.4\, h. \tag{1}$$

To judge about the particle damper's efficiency the effective loss factor $\bar{\eta}$ [6, 11] is used. It is calculated by a scaling of the dissipated energy of the particle damper per radian E_{diss} with the kinetic energy of the particle system using the mass of the particle bed m_{bed}, i. e. the mass of all particles, to

$$\bar{\eta} = \frac{E_{\text{diss}}}{E_{\text{kin}}} = \frac{E_{\text{diss}}}{\frac{1}{2}\, m_{\text{bed}}\, V^2}. \tag{2}$$

Scattered state: The scattered state occurs for container amplitude $X < X_{\text{opt}}$. This motion mode is similar to the gaslike state observed by Sack [15] under the condition of weightlessness. The particle movement is randomly and chaotic. Hence, in Fig. 1 just a schematic representation of the movement of the particles is shown. Particles are hitting each other and the container walls at random phases. In [12] it is observed that a higher vibration amplitude X leads to more particle collisions while a higher clearance h leads to fewer particle collisions.

The analytical solution of the effective loss factor of the scattered state is shown in Fig. 3 for $X < X_{\text{opt}}$ being a good approximation to experimental measurements [12]. The effective loss factor starts close to zero for very low container amplitudes, i. e. $X \ll X_{\text{opt}}$, and increases linearly. At the transition to the rolling collect-and-collide motion mode, i.e. at $X = X_{\text{opt}}$, the highest value of 0.4 is reached.

Rolling collect-and-collide: The second motion mode observed for low frequency horizontal vibrations is the rolling collect-and-collide one, see also Fig. 1 and Fig. 2. Within this motion mode, i. e. for $X > X_{\text{opt}}$, the particle bed rolls and slides as one single particle block over the container's base. Thus, the translational and rotational velocities of every single particle are assumed to be identical. First, the particle bed is pushed by the container until the container reaches its maximum velocity, i. e. at $\Omega t = n\pi$ with $n \in \mathbb{N}$. At this time point the container is positioned at $x_c = 0$ and its velocity is maximal, i. e. $\dot{x}_c = \pm V$. As the particle bed is pushed by the container, almost no rotational movement of the particles is seen during this pushing phase, i. e. $\dot{\varphi}_p = 0$. When the particle container has reached its maximum velocity and starts to decelerate, the particle block leaves the

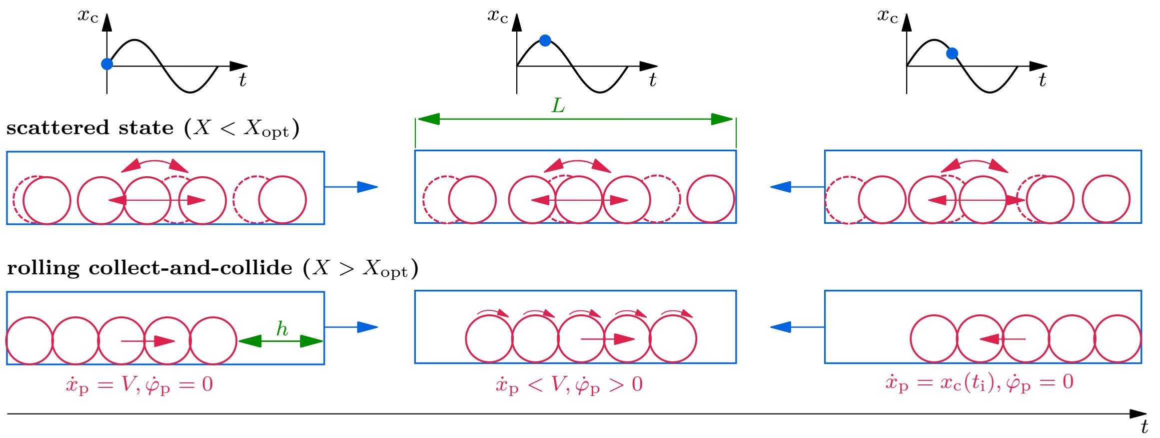

Figure 1: Motion modes at different container strokes for low acceleration amplitudes.
($\dot{x}_c$: container velocity, $\dot{x}_p$: particle bed velocity, $\dot{\varphi}_p$: angular velocity of particles)

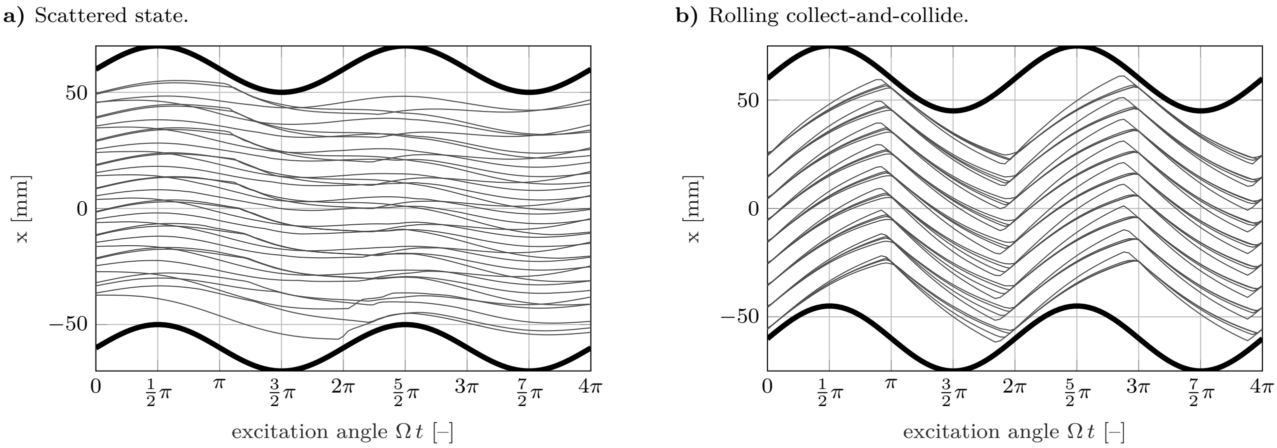

Figure 2: Particles trajectories obtained from DEM simulations for different container strokes [12].

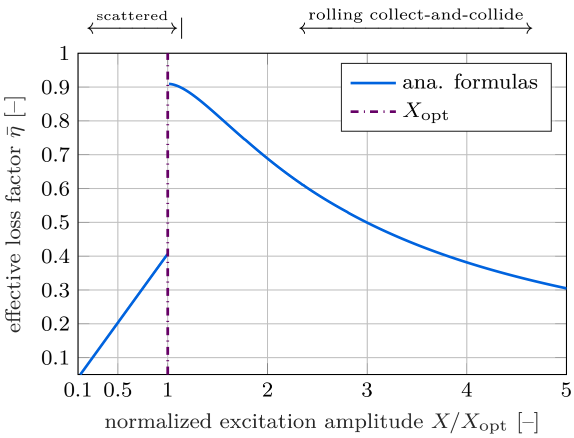

Figure 3: Effective loss factor for scattered and rolling collect-and-collide motion mode [12].

container wall and the single particles start rolling due to friction with the container base. The particle block collides inelastically with the opposite container wall at the impact time point t_{i}. During this impact multiple inter-particle and particle–wall impacts occur. Although, by every single impact, only a small amount of energy is dissipated, in sum a perfectly inelastic collision of the particle bed with the container wall is achieved, i. e. the particle block adopts the velocity of the container [1, 17]. During this inelastic collision, the rotational movement of the particles stops. This sequence is repeated when the particle container moves in the other direction. Hence, in sum, two particle impacts with the container walls occur during one vibration cycle.
The effective loss factor for this motion mode is shown in Fig. 3 for $X > X_{\mathrm{opt}}$. The effective loss factor starts at $X = X_{\mathrm{opt}}$ with its maximum value $\bar{\eta}_{\mathrm{max}} \approx 0.91$ and decreases slowly to higher container amplitudes. This progression of the effective loss factor can be explained by taking the relative velocity between particle bed and container at the impact time point with the container wall into consideration. For very high container amplitudes, i. e. $X \gg X_{\mathrm{opt}}$, the particle bed leaves the container wall with a high velocity. Thus, the particle bed collides after a short period with the opposite container wall, i.e. $\Omega\, t_{\mathrm{i}} \rightarrow 0$. Consequently, the relative velocity between particle bed and container at impact is comparatively low, resulting in a low efficiency. When the container amplitude decreases, i. e. is getting closer to X_{opt}, the impact time point increases, and thus the relative velocity at impact increases as well. This leads to a higher damper efficiency. The threshold for this motion mode is at an impact time point of $\Omega\, t_{\mathrm{i}} = \pi$. For this time point, the container is located at $x_{\mathrm{c}} = 0$ but moves in the other direction as the particle block, i. e. $\dot{x}_{\mathrm{c}} = \mp V$. This is the impact time point of maximum relative velocity between particle bed and container and thus of the highest efficiency. For this time point, $X \approx 0.4\, h$ holds. For even lower container strokes, the system switches to the scattered state. This switch happens as for the rolling collect-and-collide motion mode less than two impacts with the container wall per vibration cycle would occur. However, this is a necessary condition of this motion mode.

One should note that the experimental results in [12] are in good agreement with the analytical solutions of the effective loss factor shown in Fig. 3. However, in [12] the testbed to subject the particle container to a sinusoidally motion is set up very precisely. It is obtained that especially a container tilt or a high friction coefficient, significantly lower the effective loss factor.

Design Guideline

To design an appropriate particle damper, at first some general points have to be discussed. At first, it is assumed that the system that should be damped is described by

$$M\ddot{x} + D\dot{x} + Kx = 0, \tag{3}$$

with mass M, structural damping D, stiffness K and particle damper position x. In [8] a detailed description is given, of how to derive this equation of motion for arbitrary structures.
For the damper design, the effective loss factor, see Fig. 3, has to be considered. As the particle damper exhibits much higher effective loss factors during the rolling collect-and-collide motion mode, this motion mode should be realized during the operation of the damper. Likewise, any free vibration of a structure with initial amplitude X_0 will decrease in amplitude over time. Hence, the particle layers should be designed such that $X_0 > X_{\mathrm{opt}}$ holds to ensure an operation within the rolling collect-and-collide motion mode. However, the question arises of how to design the particle layers, i. e. particle mass and clearance h, appropriately.
In the first step, the necessary particle mass needs to be determined. It can be calculated by the desired damping ratio of the structure ζ_{d} and the effective loss factor, see [9]. However, the effective loss factor is not known and changes over time. Experimental measurements, as discussed later, have shown that an appropriate designed particle damper exhibits an effective loss factor of about $\bar{\eta} = 0.5$ on a large amplitude range. So this is a good starting value for design. The particle mass is obtained to

$$m_{\mathrm{bed}} \approx 2\,M\,\frac{\zeta_{\mathrm{d}}}{\bar{\eta}}. \tag{4}$$

Many experimental measurements, see [8], have shown that a separation of the particle container into at least three layers leads to good damping properties. To ensure a high damping over a large vibration amplitude range, the damper layers should be designed such that

$$\frac{X_0}{X_{\mathrm{opt}}} = \{2, 4, 6\}\,, \tag{5}$$

see also Fig. 3. Inserting Eq. (5) into Eq. (1) the clearances of the three damper layers are obtained to

$$h = \left\{\frac{5}{4}, \frac{5}{8}, \frac{5}{12}\right\} \cdot X_0. \tag{6}$$

Hence, starting from an initial vibration amplitude X_0, the effective loss factors are $\bar{\eta}_0 = \{0.69, 0.38, 0.25\}$ and are increasing as the vibration amplitude decreases until the optimal strokes of the individual damper layers are reached. When the optimal stroke of a layer is reached, the particle bed within this layer switches to the scattered state, and the energy dissipation of this layer reduces dramatically. The three optimal strokes are obtained by Eq. (5) to

$$X_{\mathrm{opt}} = \left\{\frac{1}{2}, \frac{1}{4}, \frac{1}{6}\right\} \cdot X_0. \tag{7}$$

Hence, the minimum vibration amplitude of the system will be about $X_{\mathrm{min}} \approx \frac{1}{6}\,X_0$ as for lower vibration amplitudes all three particle layers will be in the scattered state. Hence, only a little amplitude reduction is achieved from that moment. To ensure uniform damping, the particle mass should be distributed evenly over the damper layers. It should be noted that lower vibration amplitudes could be reached if additional damper layers are used with a higher ratio of $X_0/X_{\mathrm{opt}} = 6$. However, for very low vibration amplitudes, the effects of friction or little container tilts are becoming more and more dominant. Hence, additional damping might be hard to realize for very low container amplitudes. See [12] for further details.
To enable the inelastic collision property of the rolling collect-and-collide motion mode, see also Sect. **Motion Modes**, in each particle layer at least three by three particles should be used. To decrease the influence of friction a high particle radius is beneficial. As particle material, steel has been proven to be very durable [9, 12].

Experimental Validation

In the following, the presented design guideline shall be validated experimentally. The used experimental setup is shown in Fig. 4. It consists of a simple beam-like structure with the particle damper mounted at its tip. The elastic length of the steel beam is 512 mm with a rectangular profile of 80 mm × 2 mm and a Young's modulus of $E = 200$ GPa. The base point of the beam-like structure is fixed and the tip consists of an additional mass and the particle container with a total weight of 1270 g. The particle container is made of polyvinyl chloride (PVC) and has a quadratic cross section with an inner edge width and height of 40 mm and a length L of 120 mm in excitation direction. The container is separated into three horizontal layers with a height of 11 mm each, as shown in Fig. 4-right. Additionally, the length of each layer can be adjusted by separation walls. The container's velocity is measured using a laser scanning vibrometer, the *PSV-500* from POLYTEC, with a sampling frequency of 250 kHz and integrated internally to obtain the output position. The measurement starts at the first zero crossing of the particle container.

For this system, the mass and stiffness for Eq. (3), follow to $M = 1.058\,\mathrm{kg}$ and $K = 143\,\mathrm{N/m}$. The eigenfrequency of the undamped system is $f_0 = \omega_0/(2\pi) = 1.85\,\mathrm{Hz}$. This numerical obtained eigenfrequency is very close to the experimental measured one with only a difference of 0.02 Hz. The structural damping parameter D is obtained from measurements and is with a value of 0.032 kg/s rather small [8, 10]. All three particle layers are filled with 16 steel spheres of 5 mm radius. Hence, a total particle weight of 196 g is used. To verify Eq. (4) for the necessary particle mass, a damping ratio $\zeta = 0.046$ should be measured with this particle setting. An initial amplitude of $X_0 = -63\,\mathrm{mm}$ with clearances according to Eq. (6) are used, i. e. $h \approx \{80, 40, 25\}$ mm. The initial acceleration is $A_0 = 8.5\,\mathrm{m/s^2} < g$. Consequently, the particle bed is in the rolling collect-and-collide motion mode from the very beginning. The three resulting optimal strokes are $X_{\mathrm{opt}} = \{32, 16, 10\}$ mm. Figure 5 shows the trajectory of the system's tip, i. e. the particle damper, and the hull curve of the undamped system. Additionally, the obtained damping ratios are depicted.

During the first vibration cycle, a damping ratio of $\zeta = 0.035$ is achieved, which increases as the container amplitude decreases. The damping ratio stays high with values around $\zeta \approx 0.046$, i. e. the desired damping ratio. Around the three optimal strokes, i. e. at container amplitudes of $X_{\mathrm{c}} = \{32, 16, 10\}$ mm, a kink towards lower damping ratios is seen. This happens as here the corresponding particle layer switches into the scattered state, leading to a reduced energy dissipation. For container amplitudes below 11 mm, only very small damping ratios of about $\zeta \approx 0.02$ are achieved. This container amplitude is close to the theoretical minimum value X_{min} with 10 mm. The low damping ratios are achieved for strokes below 11 mm because all three particle layers are in the scattered state from that moment. In summary, for this system, the design guideline has been proven to be very efficient.

Sensitivity analyses: To prove that the design guideline also works efficiently for other systems, the beam-like structure is modified. The same initial amplitude, the same particle mass and the same clearances are used. For the first modification, an additional mass of 942 g is mounted at the tip. Its total mass is hence $M = 2.0\,\mathrm{kg}$. The new eigenfrequency of this system results in $f_0 = 1.35\,\mathrm{Hz}$. Due to the higher system mass, the achievable damping ratio according to Eq. (4) reduces to $\zeta = 0.025$. The experimental results of the container stroke and damping ratios are shown in Fig. 6. The results show the same qualitative behavior as for Fig. 5, but on a larger time scale, due to the higher system mass. The measured damping ratios are around $\zeta \approx 0.025$. Hence, the design guideline works still efficiently for this system.

For a second modification, a different beam is used. This steel beam has the same length but with a rectangular profile of 80 mm × 3 mm instead of 80 mm × 2 mm. This significantly changes the stiffness to $K = 484\,\mathrm{N/m}$. The system's mass is only a little affected, i. e. $M = 1.108\,\mathrm{kg}$. The system's eigenfrequency follows to $f_0 = 3.33\,\mathrm{Hz}$. Due to the increases eigenfrequency of the system, the acceleration at the initial stroke X_0 increases to $A_0 = 28\,\mathrm{m/s^2} > g$. This causes the system to be in the bouncing collect-and-collide motion mode first [8]. Here, the particles are flying thru the container instead of rolling. Indeed, the optimal stroke is only little affected as it is achieved to $X_{\mathrm{opt}} \approx 0.32\,h$ compared to $X_{\mathrm{opt}} \approx 0.4\,h$. The maximum effective loss factor value is $\bar{\eta}_{\mathrm{max}} \approx 1.27$ compared to $\bar{\eta}_{\mathrm{max}} \approx 0.91$. In Fig. 7 the trajectory of the system's tip and the damping ratios are depicted. Again, the results show similar qualitative behavior as for Fig. 5. Although the theoretical maximum effective loss factor is higher, the damping ratios are very similar compared to Fig. 5. Probably, the container layers hinder the deployment of a purely flying particle state. Indeed, this requires further investigations. Still, the design guideline even works well for container accelerations above the gravitational constant.

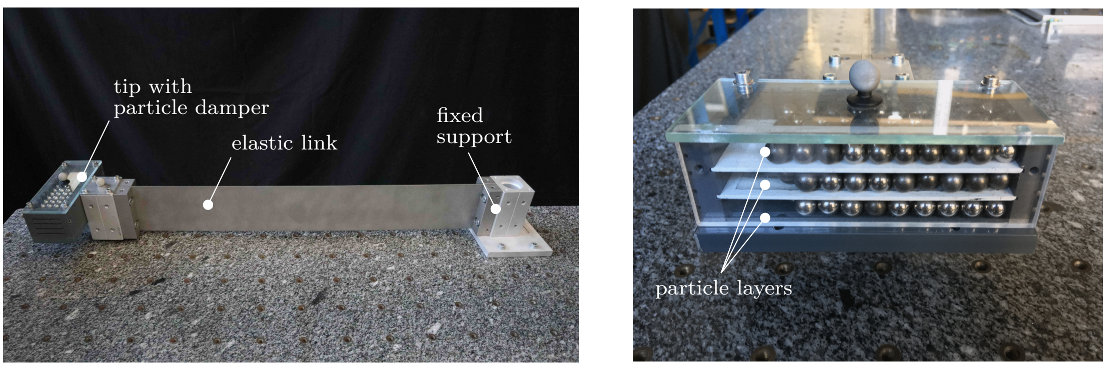

Figure 4: Simple beam-like structure setup with overview (left) and augementation of its tip (right).

a) Trajectory of tip.

b) Damping ratios.

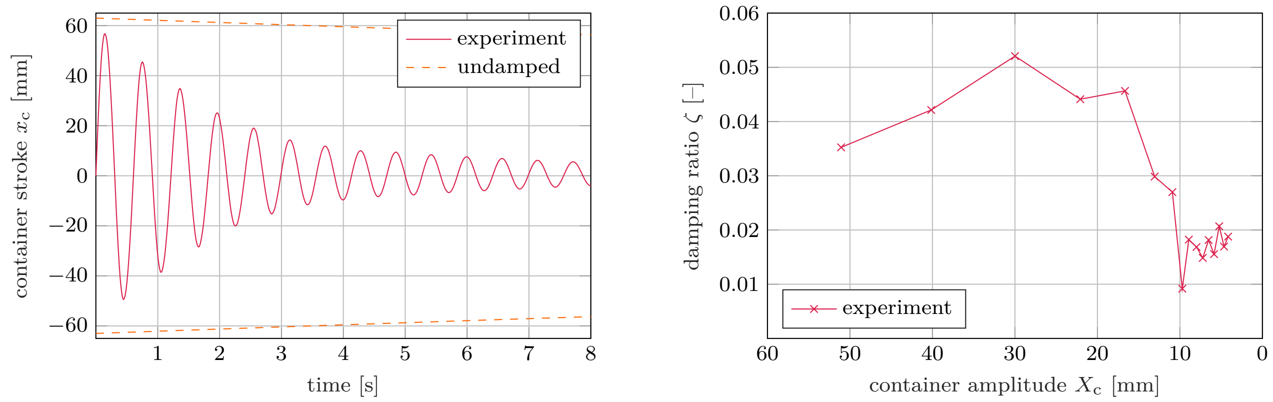

Figure 5: Damped simple beam-like structure with clearances according to Eq. (6) with **a)** trajectory of tip and **b)** damping ratios.

a) Trajectory of tip.

b) Damping ratios.

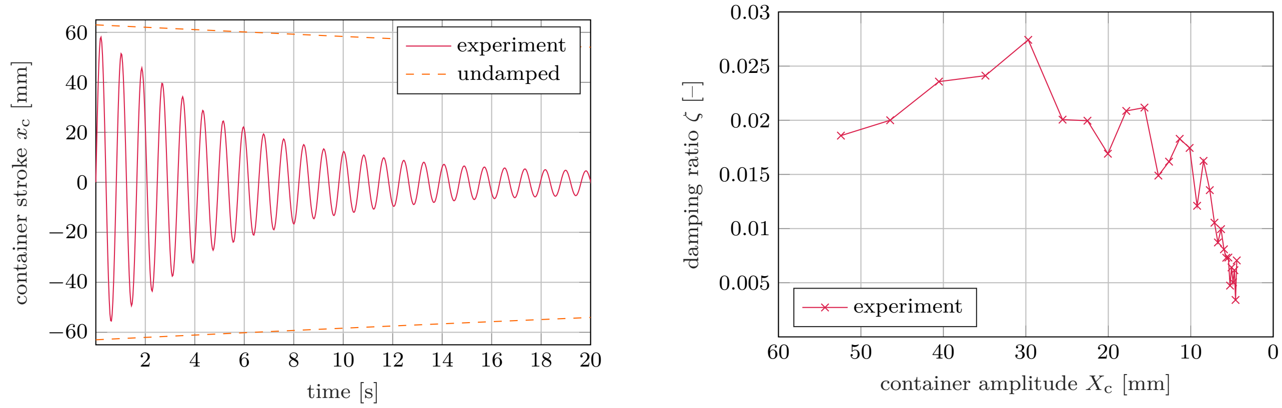

Figure 6: Damped simple beam-like structure with extra mass with **a)** trajectory of tip and **b)** damping ratios.

a) Trajectory of tip.

b) Damping ratios.

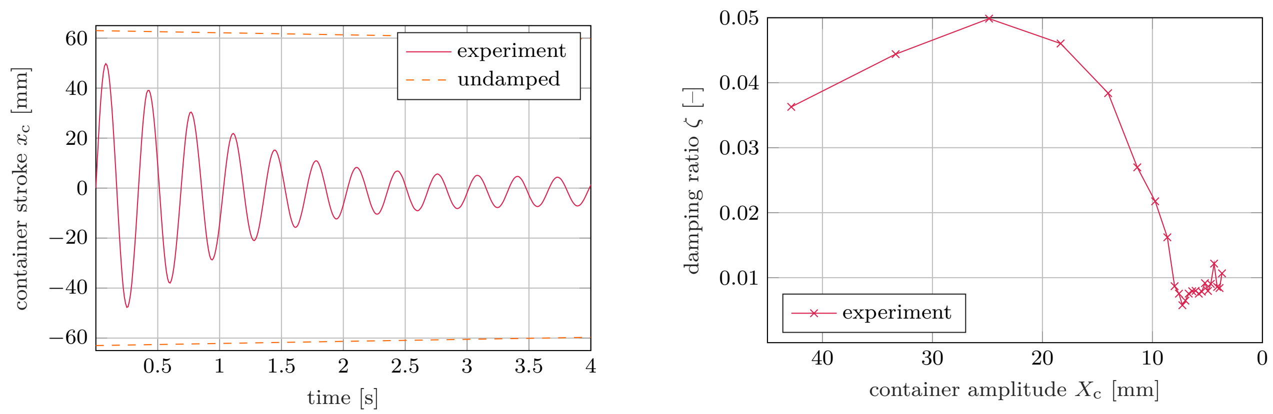

Figure 7: Damped simple beam-like structure with stiffer beam with **a)** trajectory of tip and **b)** damping ratios.

Conclusion

In this paper, a systematic design guideline for the development of layerd particle dampers for low frequency horizontal free vibrations is presented. Hereby, the rolling collect-and-collide motion mode of the particle bed is employed. The particle damper is separated into multiple particle layers and filled with steel spheres. Via the design guideline, the necessary particle mass for the desired damping ratio is determined only based on the structure's mass. A simple analytical equation is given to design the clearances of the different particle layers, i. e. the distances between the particle bed and the opposite container wall.
The efficiency of the design guideline is verified experimentally. A simple beam-like structure is used for this task. The structure is subjected to an initial deflection and the damping ratio of the free vibration is measured. The damping ratios are close to the designed values. Finally, sensitivity analyses are performed by changing either the stiffness of the beam or by adding mass. Either way, the good damping performance is conserved.

Acknowledgements

The authors would like to thank the German Research Foundation (DFG) for the financial support of the project 424825162. The authors would also like to thank Dr.-Ing. Marc-André Pick, Dipl.-Ing. Riza Demir, Dipl.-Ing. Norbert Borngräber-Sander and Wolfgang Brennecke for helping to design and realize the experimental rig.

References

[1] Bannerman, M.N., Kollmer, J.E., Sack, A., Heckel, M., Mueller, P., Pöschel, T.: Movers and shakers: Granular damping in microgravity. Physical Review E **84** (2011). DOI 10.1103/PhysRevE.84.011301

[2] Chen, T., Mao, K., Huang, X., Wang, M.: Dissipation mechanisms of nonobstructive particle damping using discrete element method. Proceedings of SPIE - The International Society for Optical Engineering **4331**, 294–301 (2001). DOI 10.1117/12.432713

[3] Eshuis, P., Weele, K., Meer, D., Lohse, D.: Granular leidenfrost effect: Experiment and theory of floating particle clusters. Physical review letters **95**, 258001 (2006). DOI 10.1103/PhysRevLett.95.258001

[4] Johnson, C.D.: Design of passive damping systems. Journal of Mechanical Design **117**(B), 171–176 (1995). DOI 10.1115/1.2838659

[5] Lu, Z., Wang, D., Masri, S., Lu, X.: An experimental study of vibration control of wind-excited high-rise buildings using particle tuned mass dampers. Smart Structures and Systems **18**, 93–115 (2016). DOI 10.12989/sss.2016.18.1.093

[6] Masmoudi, M., Job, S., Abbes, M.S., Tawfiq, I., Haddar, M.: Experimental and numerical investigations of dissipation mechanisms in particle dampers. Granular Matter **18**(3), 71 (2016). DOI 10.1007/s10035-016-0667-4

[7] Matchett, A.J., Yanagida, T., Okudaira, Y., Kobayashi, S.: Vibrating powder beds: A comparison of experimental and distinct element method simulated data. Powder Technology **107**(1), 13–30 (2000). DOI 10.1016/S0032-5910(99)00080-7

[8] Meyer, N., Schwartz, C., Morlock, M., Seifried, R.: Systematic design of particle dampers for horizontal vibrations with application to a lightweight manipulator. Journal of Sound and Vibration **510**, 116319 (2021). DOI 10.1016/j.jsv.2021.116319

[9] Meyer, N., Seifried, R.: Damping prediction of particle dampers for structures under forced vibration using effective fields. Granular Matter **23**(3), 64 (2021). DOI 10.1007/s10035-021-01128-z

[10] Meyer, N., Seifried, R.: Optimal design of particle dampers for structures with low first eigenfrequency under forced vibration. 7th edition of the International Conference on Particle-based Methods **7** (2021). DOI 10.23967/particles.2021.022

[11] Meyer, N., Seifried, R.: Toward a design methodology for particle dampers by analyzing their energy dissipation. Computational Particle Mechanics **8**(4), 681–699 (2021). DOI 10.1007/s40571-020-00363-0

[12] Meyer, N., Seifried, R.: Energy dissipation in horizontally driven particle dampers of low acceleration intensities. Nonlinear Dynamics (2022). DOI 10.1007/s11071-022-07348-z

[13] Panossian, H.: Structural damping enhancement via non-obstructive particle damping technique. Journal of Vibration and Acoustics **105**(114), 101–105 (1992). DOI 10.1115/1.2930221

[14] Panossian, H.: Non-obstructive particle damping experience and capabilities. Proceedings of SPIE - The International Society for Optical Engineering **4753**, 936–941 (2002). DOI 10.2514/6.2008-2102

[15] Sack, A., Heckel, M., Kollmer, J., Zimber, F., Pöschel, T.: Energy dissipation in driven granular matter in the absence of gravity. Physical review letters **111** (2013). DOI 10.1103/PhysRevLett.111.018001

[16] Saluena, C., Esipov, S.E., Poeschel, T., Simonian, S.S.: Dissipative properties of granular ensembles. Proceedings of SPIE **3327**(1), 23–29 (1998). DOI 10.1117/12.310696

[17] Sanchez, M., Rosenthal, G., Pugnaloni, L.: Universal response of optimal granular damping devices. Journal of Sound and Vibration **331**(20), 4389–4394 (2012). DOI 10.1016/j.jsv.2012.05.001

[18] Simonian, S.S.: Particle beam damper. Proceedings of SPIE - The International Society for Optical Engineering **2445**, 149–160 (1995). DOI 10.1117/12.208884

[19] Wong, C.X., Daniel, M.C., Rongong, J.A.: Energy dissipation prediction of particle dampers. Journal of Sound and Vibration **319**(1-2), 91–118 (2009). DOI 10.1016/j.jsv.2008.06.027

[20] Yin, Z., Su, F., Zhang, H.: Investigation of the energy dissipation of different rheology behaviors in a non-obstructive particle damper. Powder Technology **321** (2017). DOI 10.1016/j.powtec.2017.07.090

[21] Zhang, K., Chen, T., He, L.: Damping behaviors of granular particles in a vertically vibrated closed container. Powder Technology **321**, 173–179 (2017). DOI 10.1016/j.powtec.2017.08.020